Prevention of Corrosion Related Failure of Aircraft Aluminum Using an Engineered Residual Stress Field

Jeremy Scheel,
Paul Prevéy and Douglas Hornbach
Lambda Technologies
5521 Fair Lane
Cincinnati, Ohio 45227-3401
jscheel@lambdatechs.com

ABSTRACT

The effect of corrosion damage on the high cycle fatigue (HCF) performance of AA7075-T6 alloy was evaluated. Corrosion fatigue specimens were processed using either a conventional 6-8A, 200% shot peening (SP) treatment or low plasticity burnishing (LPB), a CNC controlled process capable of being performed robotically 'on wing' as well as with conventional CNC machine tools. Stress vs. life corrosion fatigue curves were established for each process; pitting depth and anodic polarization studies were also performed.

Residual stress measurements were performed to quantify the magnitude and depth of residual compression from each process. LPB imparted a depth of compression 3X greater than SP without the severe cold working produced by SP. The corrosion fatigue life for LPB specimens was increased by greater than an order of magnitude over SP. Pit depths were measured as a function of time and were found to approach a maximum depth dependent upon the surface treatment used. Anodic polarization testing revealed a shift in the open circuit potential (OCP) of nominally 0.12 V between SP and LPB treated specimens. The LPB specimens were found to be nobler, having a lower OCP than the SP specimens.

Corrosion damage exceeding the depth of compression on a component served as the nucleation point(s) for corrosion induced fatigue cracking. A deep, stable layer of engineered residual compression can successfully mitigate corrosion damage and greatly increase corrosion fatigue life.

Keywords: Corrosion Fatigue, Pitting, Stress Corrosion Cracking (SCC), High Cycle Fatigue (HCF), Low Plasticity Burnishing (LPB), Shot Peening (SP) Compressive Residual Stress.

Introduction:

The many aircraft that have been designated to be retired and replaced will need to continue operation for an extended period of time. It is imperative that the existing fleet of aging aircraft continues to operate safely and at full capacity while remaining cost effective. Current annual cost for corrosion inspection and repair of military aircraft alone are estimated to exceed one billion dollars annually. More than 30% of military aircraft are over 20 years old, and over 90% are expected to exceed a 20-year life by the year 2015. The total cost of ownership and fleet readiness are adversely affected at an increasing rate. A means of mitigating corrosion and corrosion-related fatigue damage is needed to prolong the service life of many structures and components as the fleet continues to age.

Surface enhancement of metals, inducing a layer of surface compressive residual stresses in metallic components, has long been recognized to enhance fatigue strength[1-4]. The fatigue strength of many engineering components is often improved by shot peening (SP). Low plasticity burnishing (LPB)[5] is an advanced process that further benefits fatigue and corrosion prone components. Maximum benefits are obtained when deep compression is achieved with minimal cold working of the surface.

Cold working is critical in military aircraft aluminum alloys that will experience a corrosive environment. It is routine practice to grind out corrosion pits and other damage from components until clean metal is reached. A SP or blasting process is then typically used prior to painting and coatings to restore the aircraft. While effective at removing damage and inducing a shallow layer of compressive residual stress, this practice induces high levels of cold working into the material, as the surface is repeatedly deformed. The high levels of cold working generate an increased dislocation density. Controlling the amount of cold working during surface enhancement allows for a stable, engineered compressive residual stress field that will not relax under thermal or mechanical stress[6].

LPB has been demonstrated to provide a deep surface layer of stable, high magnitude compression with controlled, low cold working typically in the 3-5% range in aluminum, steel, titanium, and nickel based super-alloys. LPB is currently used in production in multiple aerospace, nuclear and medical applications, including military gas turbine engine blades and vanes and the propeller taper bore for the P-3 Orion. The low amount of cold working from LPB ensures thermo-mechanical stability and the deep compression induced mitigates fatigue damage including FOD[7-9], fretting[10-12], SCC, and corrosion[12-15]. The LPB process is a ‘turn key’ technology performed on conventional CNC machine tools or robots, compatible with the overhaul or depot shop environment as well as production facilities. LPB has been accepted by the FAA for commercial aircraft maintenance, repair and alteration to improve fatigue and SCC performance of aircraft components including engine, landing gear, and structural components.

Corrosion pits from salt spray are common sites of fatigue crack initiation in aircraft aluminum alloy structures. Corrosion pitting occurs during exposure to a marine atmosphere and results in corrosion to a depth depending on the time of exposure, temperature, and the service environment. The pronounced fatigue strength reduction caused by corrosion pitting is well established for aluminum alloys, and typically reduces the endurance limit to nominally half of the un-corroded value. The depth of compression is critical in preventing failure from corrosion pits. If the overall depth of compression exceeds the depth of pitting then fatigue failure from

pitting is mitigated[16]. An overview of test results from studies on aluminum alloy AA7075-T6 is presented in this paper. The effects of SP and LPB on active corrosion fatigue and the fatigue performance after salt fog and / or SCC exposure are shown. The role of cold working and its resultant effect on the open circuit potential of treated surfaces is presented.

EXPERIMENTAL PROCEDURE

Material

AA7075-T6 material was acquired in plate form and machined into test specimens. Table I shows material and chemistry properties that were verified prior to machining of specimens. Two specimen geometries were used in testing. Specimen Type 1 consists of rectangular bars with an undercut trapezoidal gage region nominally 8 x 1.25 x 3/8 in. (203 x 32 x 9.5 mm) used for HCF/SCC testing. The trapezoidal cross section HCF sample was designed to force the fatigue failures to initiate in the compressive gage section surface under 4-point bend loading. Specimen Type 2 was a square coupon, nominally 2 x 2 x 3/8 in. thick (50.8 x 50.8 x 9.5 mm) used for pitting and anodic polarization testing.

CHEMICAL PROPERTIES

Element	***Plate Analysis (Wt %)***	***AMS 4045 Limits***
Zn	5.5	5.1-6.1
Mg	2.44	2.1-2.9
Cu	1.45	1.2-2.0
Fe	0.25	0.7 max
Cr	0.19	0.18-0.40
Si	0.07	0.50 max
Ti	--	0.20 max
Mn	--	0.30 max
Al	Remainder	Remainder
MECHANICAL PROPERTIES		
UTS	***0.2% Y.S.***	***ELONGATION***
87.3 ksi (601 MPa)	78.7 ksi (542 MPa)	11% uniform

Table I: AA7075-T6 Chemical and Material Properties.

Specimen Processing

Surface enhancement of specimens was performed using a conventional SP process or by LPB processing. Each process is discussed in brief below.

Low Plasticity Burnishing (LPB):

LPB process parameters were developed for both specimen types to introduce the appropriate depth or compression with low cold working. CNC control code was created to allow positioning of the LPB tool in a series of passes along the region to be processed while controlling the burnishing pressure to develop the pre-determined magnitude of compressive stress with controlled low cold working. The LPB process has been described in previous publications.

Shot Peening (SP):

Shot peening was performed using a conventional air blast peening system equipped with a rotating table on both specimen types with the following process parameters: 200% coverage and CCW14 shot; 6-8A Almen intensity. Specimens were examined optically under low magnification to confirm coverage.

High Cycle Fatigue Testing

High cycle fatigue (HCF) tests were performed under constant amplitude loading on a Sonntag SF-1U fatigue machine. Fatigue testing was conducted at ambient temperature ~72°F (~22°C) in four-point bending mode[17]. The cyclic frequency and stress ratio, R ($\sigma_{min}/\sigma_{max}$), were 30 Hz and 0.1 respectively. Tests were conducted to specimen fracture or until a "run-out" life of 1 x 10^7 cycles was attained, whichever occurred first. Testing was terminated upon specimen failure. Specimens were subsequently broken fully open, if not cracked through entirely, to permit direct observation of fracture surface details using optical and SEM analysis. Several corrosive test methods were used to damage the specimens prior to and during HCF testing to fully evaluate the benefits of both surface treatments tested.

Active Corrosion (AC)

Active corrosion (AC) fatigue testing was performed in a medium of neutral 3.5% NaCl salt solution prepared with de-ionized water. Filter papers were soaked with the solution, wrapped around the gage section of the fatigue test specimen, and sealed with a plastic film to avoid evaporation.

Salt Fog Corrosion Exposure

A salt fog corrosion exposure was performed at 35° C per ASTM B117, Standard Practice for Operating Salt Spray (Fog) Apparatus. The fog produced was such that 1.0-2.0 ml/hr of 5 $\pm$ 1 mass percent NaCl aqueous solution collected on each 80 cm^2 horizontal surface. The pH of the solution was maintained between 6.5 and 7.2. The salt fog exposure was performed at the Naval Air Depot at Cherry Point using a model TTC600 chamber manufactured by Q-Fog Corporation.

The specimens were exposed in two groups with the test surface horizontal for 100 and 500 hours. Following exposure to the salt fog, the samples were soaked and then rinsed in tap water, followed with a distilled water rinse to remove any salt solution remaining, and then dried. Patches of gray and white corrosion product evident on the surface of the samples were identified by x-ray diffraction as α- Al_2O_3. The corrosion product was not removed prior to testing or LPB processing.

Stress Corrosion Cracking (SCC)

Specimens were HCF tested with and without prior exposure to SCC damage to determine the effect on the fatigue life. Stress corrosion cracking exposure tests were conducted according to ASTM Standard G 39 and G44-99. All exposed specimens were loaded in tension to 65.7 ksi, 90% of the yield strength, in 4-point bending using specially designed fixtures; the loads on the

specimens were monitored using instrumented bolts. Specimens were exposed to 3.5% NaCl salt solution by alternate immersion (10 minutes in and 50 minutes out per cycle). The load history on each specimen was monitored for 100 hours at which point the specimens were removed, cleaned with water, and tested in HCF. Specimens were tested in isolated baths specific to the material to avoid any possible galvanic effect during the SCC exposure.

Maximum Pit Depth Testing

Alternate immersion testing was conducted per ASTM G44 in neutral 3.5 weight% NaCl solution at a constant temperature of 90°F (32°C) to determine the pit depth as a function of time. Specimen Types 1 and 2 were tested in the following conditions: SP, and LPB processed. Testing was conducted using an automated alternate immersion tank. Samples were immersed in solution for 10 minutes and exposed to air for 50 minutes of a 1-hour cycle. A specimen of each surface treatment was removed and evaluated periodically. Samples were cleaned and preserved in a sealed storage bag with silica gel desiccant to ensure no further corrosion in storage. Pit depths were measured using a Zeiss optical microscope at a magnification of 320X. Pit depths were plotted as a function of exposure time.

Anodic Polarization Testing

To characterize the effect of cold working from the SP and LPB treatments on the corrosion properties of 7075-T6, anodic polarization curves were generated for each material. A custom electrochemical cell based on the Avesta Cell was used in testing. The cell is designed to prevent crevice corrosion of the specimen during testing. The OCP was recorded as a function of cold working. Specimens were also tested in a fully electropolished condition with 0% cold working. Anodic polarization testing was performed in an electrochemical cell modified to eliminate the effect of crevice corrosion in order to make more accurate observations of the OCP and electrochemical behavior of the materials. All testing was performed in a neutral solution of 3.5% weight sodium chloride and distilled water according to the guidelines of ASTM G-5. A saturated calomel electrode (SCE) was used as the reference electrode and platinum was used as the counter electrode. Testing was performed under both aerated and nitrogen purged conditions. All specimens were tested at 25° C and were pickled for 1 hour prior to measurement.

X-ray Diffraction Residual Stress and Cold Work Measurement

X-ray diffraction residual stress and cold work measurements were made at the surface and at several depths below the surface on LPB and SP treated fatigue specimens. Measurements were made in the longitudinal direction in the gage region employing a $\sin^2\psi$ technique and the diffraction of chromium $K\alpha_1$ radiation from the (311) planes of Aluminum[18]. The cold work is calculated using an empirical relationship between the diffraction peak width and percent cold work.

Material was removed electrolytically for subsurface measurement in order to minimize possible alteration of the subsurface residual stress. The measurements were corrected for both the penetration of the radiation into the subsurface stress gradient and for stress relaxation caused by layer removal[18-20]. The value of the x-ray elastic constants required to calculate the macroscopic residual stress from the strain normal to the (311) planes of aluminum were

determined in accordance with ASTM E1426-9[21]. Systematic errors were monitored per ASTM specification E915.

EXPERIMENTAL RESULTS

High Cycle Fatigue Testing

Stress vs. Life (S-N) curves were generated for the various corrosive conditions detailed above. Each surface treatment was initially tested in a 'baseline' condition, with no prior or active corrosion damage, to determine the full fatigue benefit of each treatment in the absence of a corrosive environment. The depth of compression in relation to the depth of the pits proved a critical factor. The greater depth of compression from the LPB process provided a much greater fatigue life particularly under corrosive damaged conditions. Damaged LPB processed specimens exhibited a fatigue life equal to or greater than, the undamaged as-machined specimens. The undamaged LPB condition produced the highest fatigue strength and longest life of all the conditions tested. When corrosive damage is introduced the shallow layer of compression from SP is quickly penetrated and failure ensues. Deep compression from LPB prevents failure from pitting and other surface damage, greatly extending the fatigue life over the SP condition.

Figure 1 shows the S-N curves for the conditions tested. Figure 2 shows the fatigue strength at 10 million cycles. The LPB process improved fatigue strength by greater than 1.5X over the SP treatment under active corrosive conditions during testing. LPB used as a repair process on as-machined + SCC exposed specimens was able to restore the fatigue life to greater than that of SP + SCC specimens. The fatigue life was improved by greater than an order of magnitude over the SP repair specimens. LPB repair processing was performed directly over the pre-corroded material with no prior cleaning other than a rinse in distilled water. The LPB process increased the fatigue life at moderate stresses by a factor greater than 100X over the SP treatment.

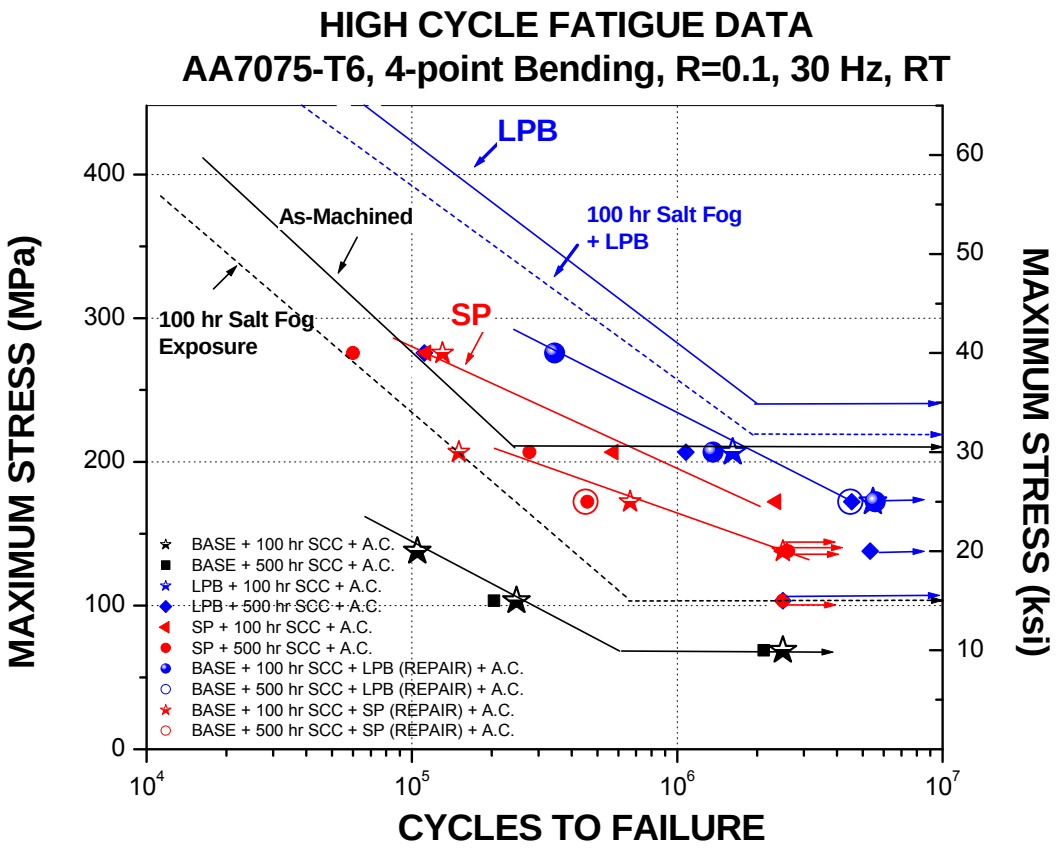

Figure 1: S-N curve for AA7075-T6. The LPB process increased the corrosion fatigue life by an order of magnitude or greater in all conditions. As a repair process LPB restored the fatigue life to greater than that of an undamaged and untreated specimen.

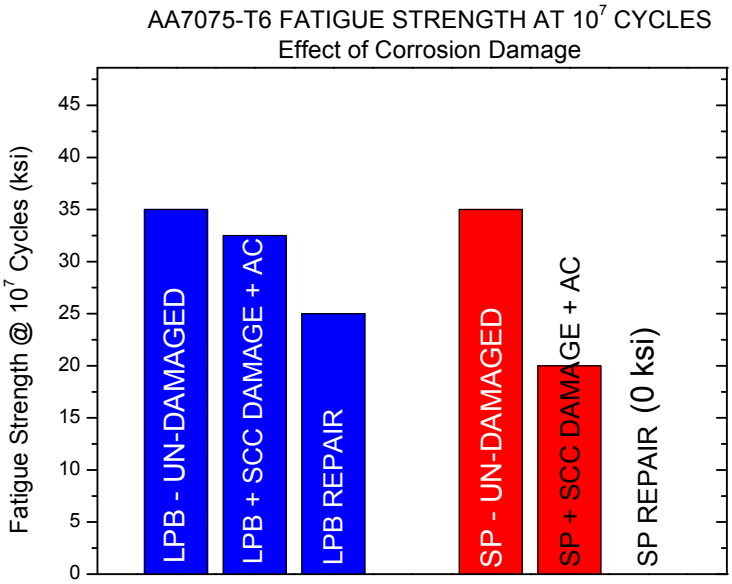

Figure 2: Comparing the fatigue strength at 10^7 cycles. LPB processed specimens demonstrated an increased strength over the SP treatment. The SP repair process failed prior to 10^7 cycles at all stresses tested.

Failure Analysis and Fractography

Fractography of failed HCF specimens was conducted using both a metallurgical optical microscope and a scanning electron microscope to reveal the nature of the fatigue failures. Fractographic analysis revealed that nearly all of the as-machined and SP processed specimens, tested under corrosive conditions, failed from one or more pits. Specimens tested at lower stresses generally exhibited failure initiation from a single deep pit or surface artifact while specimens tested at higher stress levels tended to have multiple nucleation sites. The LPB specimens failed either at the surface or had subsurface initiations. Failure initiation from pits was not observed in the LPB treated specimens. This can be attributed to the greater depth of compression from LPB. The pits did not exceed the compressive layer and did not serve as failure initiations.

Max Pit Depth Testing

Figure 3 shows the maximum pit depth vs. exposure time found for either process compared to the depth of compression imparted. It was observed from the pit depth vs. time plot that the pit depth asymptotically approaches a maximum depth. The maximum pit depth was nominally 18.7 x 10^{-3} in. (0.475 mm). LPB produced a depth of compression over 2X greater than the max pit depth observed. By introducing compression deeper than the maximum pit depth the HCF damage tolerance was dramatically improved as shown above.

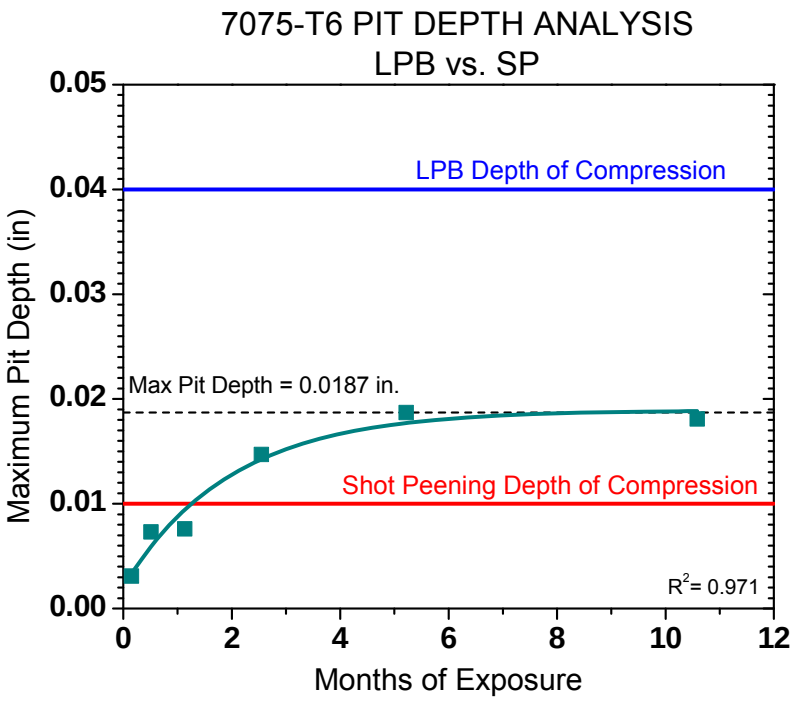

Figure 3: Max pit depth as a function of time. LPB had ~ 2X greater depth than the deepest pits. Pit depths exceeded SP depth of compression and reduced fatigue performance was evident as a result.

Anodic Polarization Testing

The results of the anodic polarization tests performed revealed a shift in the OCP of the specimens that is dependent on the percent cold work. Specimens were tested with varying degrees of cold working to observe the change in OCP. The OCP (V, SCE) and current density (A/cm^2) both increased as a function of increasing cold work. This implies greater electrochemical activity at the surface of highly cold worked material and results in a greater propensity to corrode at a faster rate. Figures 4 and 5 show the anodic polarization curves and a linear fit of the OCP vs. cold work for AA7075-T6. The amount of cold working is indicated for each surface treatment.

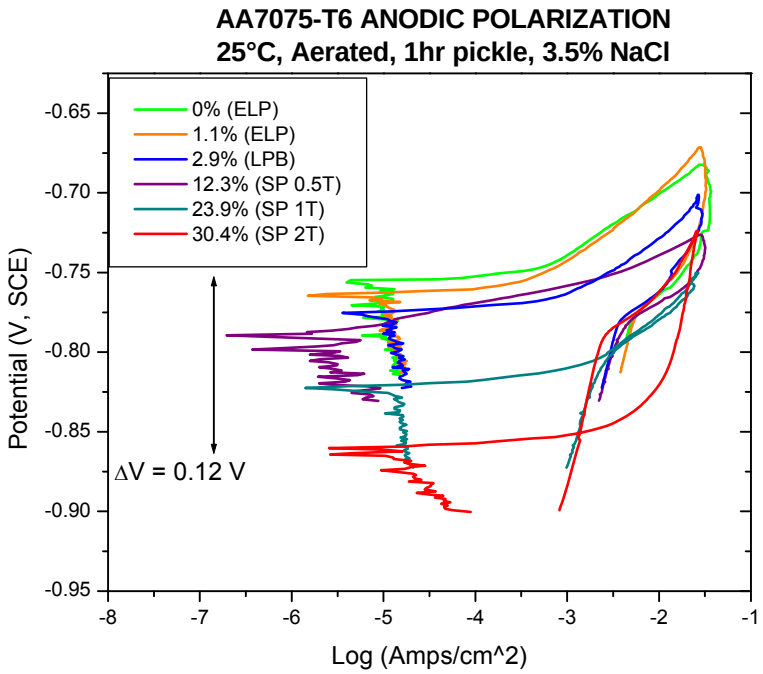

Figure 4: Anodic polarization testing of AA7075-T6. The surface treatment and resulting percent cold work is shown in the legend. As the percent cold working decreases the OCP becomes nobler, decreasing the corrosion rate.

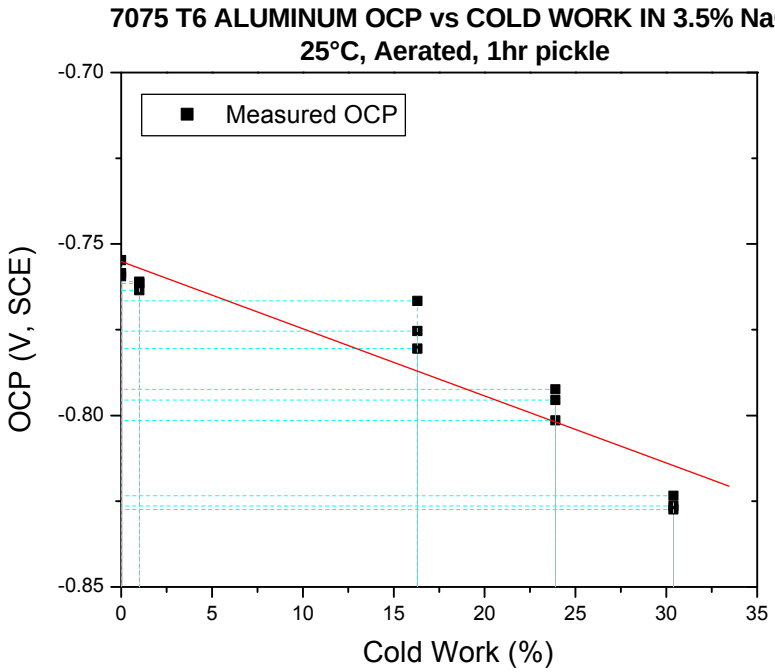

Figure 5: Linear fit of the OCP vs. percent cold work for AA7075-T6. Three repeat measurements were made at each cold work percentage tested.

The 200% (2T) SP process produced the highest percent cold work with nominally 30.4%. The electropolished specimens had 0% cold working after removal of 0.010 in. from the surface. The LPB process generated an average of nominally 2.4% cold working. The change in OCP between the 30.4% cold work and 0% cold work was nominally 0.12 V, SCE.

Figure 6 shows a macro photograph of a ½ LPB treated and ½ SP specimen's surface after polarization testing. Specimens were evaluated for corrosion damage microscopically after testing, and a greater pitting density and depth was observed on the highly cold worked specimens. The SP half of the exposed area suffered the majority of pitting and corrosion damage while cathodically protecting the lower cold worked LPB surface which suffered only minor discoloration with no pitting of any substantial depth.

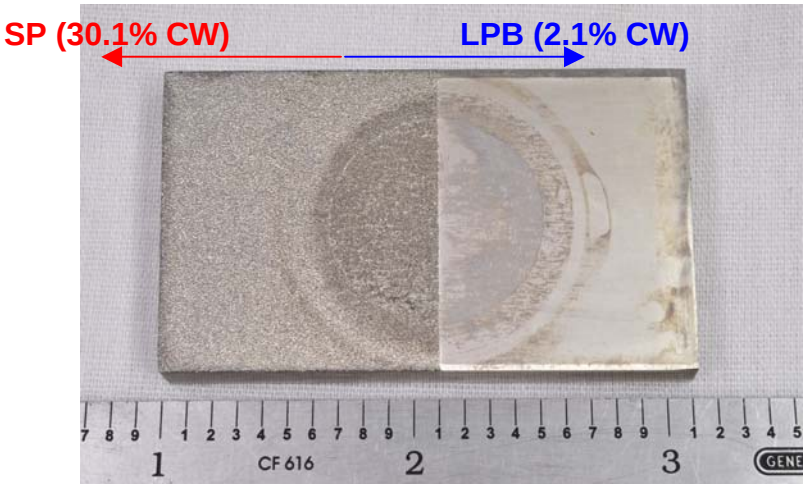

Figure 6: ½ SP ½ LPB AA7075-T6 coupon after anodic polarization testing in 3.5% NaCl purged with N_2. The highly cold worked SP area was pitted and corroded while the low cold worked LPB area was discolored with minor pitting.

To further evaluate this observation a battery was created from AA7075-T6 coupons that were LPB processed on one side and SP processed on the other. Figure 7 shows the AA7075-T6 battery setup. Filter paper pads were soaked with a 3.5% weight NaCl solution. A voltmeter was used to measure the resulting voltage when the specimens were placed together with the filter paper in between each specimen. It was found that each individual specimen produced approximately 0.1 V. Each specimen behaved as a galvanic couple due to the difference in cold work from one side to the other. Ten (10) specimens were stacked together and a resulting voltage equal to 1 V was recorded on the voltmeter. The SP surfaces of the battery cell showed characteristic pitting and general corrosion while the LPB processed side showed little damage at all.

The galvanic behavior observed could be put to practical use in aircraft aluminum by intentionally performing surface treatments that produce high cold working in non-critical areas or components and using a low cold work process such as LPB to process critical regions. As discussed above the difference in percent cold work will galvanically protect the areas with low cold working.

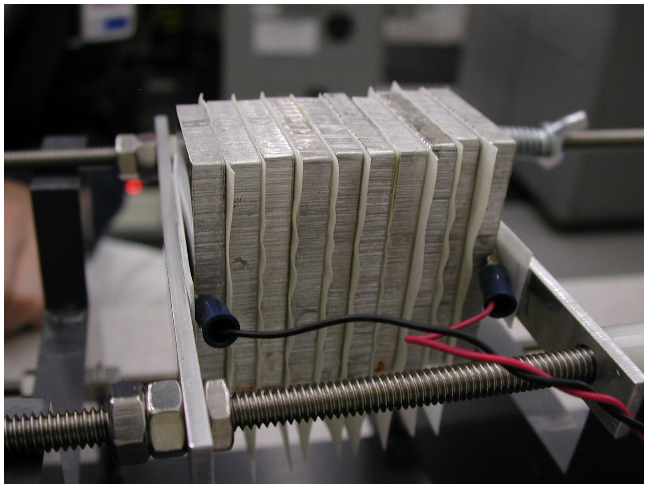

Figure 7: AA7075-T6 Battery test setup. A voltage of 1 V was generated by the galvanic behavior induced by the cold work differential.

Residual Stress Distributions

X-ray diffraction results for AA7075-T6 HCF specimens are presented graphically in Figure 8. Compressive stresses are shown as negative values, and tensile stresses as positive, in units of ksi (10^3 psi) and MPa (10^6 N/m^2). Compared to SP, LPB processing produced a compressive residual stress field with an 18% greater magnitude of compression and over 3X the depth of compression. The random impact of shot during the SP process created multiple impacts at the same location on the specimens. This repeated plastic deformation produced high cold working in SP treated specimens leading to the increased electrochemical activity as well as instability under thermo-mechanical stressing. The LPB process produced much less cold working than SP ensuring the deep compression remains stable, even at elevated temperature. The depth of compression from the LPB process greatly exceeds the average pit depth observed, preventing fatigue crack initiation from pits shallower than the compressive field. This result is reflected in the improved fatigue performance and more noble OCP values shown above.

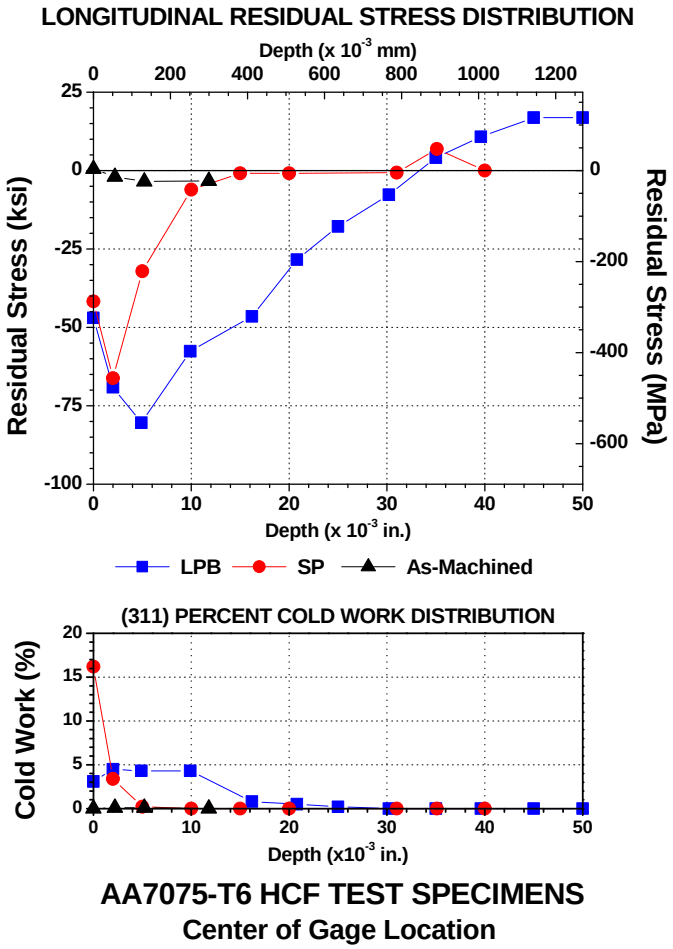

Figure 8: Residual stress distributions for each surface treatment on AA7075-T6. LPB processing provided greater magnitude and greater than 3X depth of compression than SP with less than 5% cold working.

CONCLUSIONS

The corrosion fatigue performance of 7075-T6 was greatly improved by the LPB process relative to shot peening (SP). Whether used as a repair process or during initial manufacture, LPB increased the fatigue life of the specimens by greater than an order of magnitude compared to SP. The depth of the compression proved to be a critical factor; the shallow depth of SP stresses was quickly penetrated by corrosion pits, resulting in fatigue failure nucleating from pits. The greater depth of compression from the LPB process mitigated the effect of the surface corrosion damage and provided a fatigue life improvement of greater than an order of magnitude over SP. When used as a repair process, LPB also provided as much as an order of magnitude improvement in fatigue life over SP.

Results from anodic polarization testing showed that the cold work from surface enhancement has an effect on the corrosion behavior. A shift in the OCP of nominally 0.12 V, SCE was observed and was determined to be a function of the percent cold work. The highly cold worked SP condition was in a more active state at the surface than the low cold worked LPB

and ELP specimens. This increases the likelihood and rate of corrosion. A battery was constructed of AA7075 to demonstrate this effect, and a voltage of 1.0 V was achieved through the galvanic reaction resulting from the cold work differential.

Fractographic analysis revealed that SP processed specimens failed predominately from single, or multiple, deep pits that exceeded the depth of compression. LPB processed specimens did not fail from pits and exhibited surface failures typical of non-corrosive fatigue failures where failure occurred simply due to reaching the fatigue limit for a particular stress.

This investigation shows that the fatigue life of commonly used aircraft aluminum alloys can be dramatically increased by use of engineered compressive residual stresses and controlled cold work. The need for frequent inspections under retirement for cause can be eliminated through use of engineered compressive residual stress. This engineered approach to safe life operation can greatly extend the operational service life of all aging aircraft, increase time-on-wing, and reduce operational costs. It is proposed that controlling the amount of cold working strategically is a viable method to protect critical components through cathodic protection without the use of dissimilar metals.

REFERENCES

1. Frost, N.E. Marsh, K.J. Pook, L.P., (1974), *Metal Fatigue*, Oxford University Press.

2. Fuchs, H.O. and Stephens, R.I., (1980), *Metal Fatigue In Engineerin*g, John Wiley & Sons.

3. Berns, H. and Weber, L., (1984), "Influence of Residual Stresses on Crack Growth," Impact Surface Treatment, edited by S.A. Meguid, Elsevier, 33-44.

4. Ferreira, J.A.M., Boorrego, L.F.P., and Costa, J.D.M., (1996), "Effects of Surface Treatments on the Fatigue of Notched Bend Specimens," Fatigue, Fract. Engng. Mater., Struct., Vol. 19 No.1, pp 111-117.

5. Prevéy, P.S., Ravindranath, Gabb, and Shepard., (2003), "Case Studies of Fatigue Life Improvement in Gas Turbine Engine Applications" Proc of the ASME Turbo Expo, Atlanta, GA. June 16-19.

6. Paul S. Prevéy, "The Effect of Cold Work on the Thermal Stability of Residual Compression in Surface Enhanced IN718", Proceedings of the 20th ASM Materials Solutions Conference and Exposition, St. Louis, MO, Oct. 10-12, 2000.

7. P. Prevéy, N. Jayaraman, R. Ravindranath, (2003), "Effect of Surface Treatments on HCF Performance and FOD Tolerance of a Ti-6Al-4V Vane," Proceedings 8th National Turbine Engine HCF Conference, Monterey, CA, April 14-16.

8. Paul S. Prevéy, Doug Hornbach, Terry Jacobs, and Ravi Ravindranath, (2002), "Improved Damage Tolerance in Titanium Alloy Fan Blades with Low Plasticity Burnishing," Proceedings of the ASM IFHTSE Conference, Columbus, OH, Oct. 7-10.

9. Paul S. Prevéy, et. al., (2001), "The Effect of Low Plasticity Burnishing (LPB) on the HCF Performance and FOD Resistance of Ti-6Al-4V," Proceedings: 6th National Turbine Engine High Cycle Fatigue (HCF) Conference, Jacksonville, FL, March 5-8.

10. M. Shepard, P. Prevéy, N. Jayaraman, (2003), "Effect of Surface Treatments on Fretting Fatigue Performance of Ti-6Al-4V," Proceedings 8th National Turbine Engine HCF Conference, Monterey, CA, April 14-16.

11. Paul S. Prevéy and John T. Cammett, (2002), "Restoring Fatigue Performance of Corrosion Damaged AA7075-T6 and Fretting in 4340 Steel with Low Plasticity Burnishing," Proceedings 6th Joint FAA/DoD/NASA Aging Aircraft Conference, San Francisco, CA, Sept 16-19.

12. N. Jayaraman, Paul S. Prevéy, Murray Mahoney, (2003), "Fatigue Life Improvement of an Aluminum Alloy FSW with Low Plasticity Burnishing," Proceedings 132nd TMS Annual Meeting, San Diego, CA, Mar. 2-6.
13. Paul S. Prevéy and John T. Cammett, (2002), "The Influence of Surface Enhancement by Low Plasticity Burnishing on the Corrosion Fatigue Performance of AA7075-T6," Proceedings 5th International Aircraft Corrosion Workshop, Solomons, Maryland, Aug. 20-23.

14. John T. Cammett and Paul S. Prevéy, (2003), "Fatigue Strength Restoration in Corrosion Pitted 4340 Alloy Steel Via Low Plasticity Burnishing" Retrieved from www.lambda-research.com Sept. 5.

15. Paul S. Prevéy, (2000), "Low Cost Corrosion Damage Mitigation and Improved Fatigue Performance of Low Plasticity Burnished 7075-T6," Proceedings of the 4th International Aircraft Corrosion Workshop, Solomons, MD, Aug. 22-25.

16. J. Scheel, P. Prevéy, D. Hornbach, “Safe Life Conversion of Aircraft Aluminums via Low Plasticity Burnishing” Proceedings of the Dept. of Defense Corrosion Conference. 2008.

17. Prevey et al., (2004) “Mitigation of SCC and Corrosion Fatigue Failures in 300M Landing Gear Steel Using Mechanical Suppression,” Proceedings of the 6th Aircraft Corrosion Workshop, Solomons, Maryland, 2004.

18. Paul S. Prevéy, "The Measurement of Subsurface Residual Stress and Cold Work Distributions in Nickel Base Alloys," Residual Stress in Design, Process and Materials Selection, ed. W.B. Young, Metals Park, OH: Am. Soc. for Metals, 1987, pp. 11-19.

19. Cullity, B.D., (1978) Elements of X-ray Diffraction, 2nd ed., (Reading, MA: Addison-Wesley), pp. 447-476.

20. Prevéy, P.S., (1986), “X-Ray Diffraction Residual Stress Techniques,” *Metals Handbook*, **10**, (Metals Park, OH: ASM), pp 380-392.

21. Koistinen, D.P. and Marburger, R.E., (1964), Transactions of the ASM, **67**